

Proton spectral functions in finite nuclei based on the extended Brueckner-Hartree-Fock approach

Pei Wang,¹ Peng Yin ^{*,2,3} Xinle Shang ^{†,2} and Wei Zuo ^{‡2,4}

¹*National Astronomical Observatories, Chinese Academy of Sciences, Beijing 100012, China*

²*Institute of Modern Physics, Chinese Academy of Sciences, Lanzhou 730000, China*

³*Department of Physics and Astronomy, Iowa State University, Ames, IA 50011, USA*

⁴*University of Chinese Academy of Sciences, Beijing, 100049, China*

We have calculated the proton spectral functions in finite nuclei based on the local density approximation where the properties of finite nuclei and nuclear matter are calculated by the Skyrme-Hartree-Fock method and the extended Brueckner-Hartree-Fock approach, respectively. The scaled spectral function from our calculation is in good agreement with experimental results at small momenta while the difference between them becomes apparent at high momenta. Besides, a target dependence of the scaled proton spectral function is also obtained in our calculation as was observed in experiment. A further investigation indicates that the proportion of the high density region of the proton has a significant contribution to this target-dependent behavior since the spectral function in asymmetric nuclear matter increases significantly as a function of density.

PACS numbers: 21.30.Fe, 21.65.+f, 24.10.Cn

I. INTRODUCTION

Nucleon-nucleon (NN) short-range correlations which are induced by the hard core in the bare NN potential are of great interest since they are closely related to the properties of neutron-rich nuclei, particle production in heavy-ion collisions, as well as neutron star physics [1–3]. It leads to a new challenge to test the validity of the physical picture of independent particle motion in the mean field theory or the standard shell model [4, 5].

In experiment, the effects of NN correlations can be investigated by the $(e, e'p)$, $(e, e'NN)$ and proton induced knock-out reactions [6–8]. The related measurements have been reported continually [9–19] and definite evidence of short-range NN correlations has been observed in these experiments. One important measurement of such medium modifications is the spectral function which can be observed in electron scattering experiments [20].

Nucleon spectral function in nuclear matter has been calculated by adopting various many-body methods, such as the relativistic Dirac-Brueckner-Hartree-Fock theory [21], the transport model [22], the in-medium T-matrix approach [23], the self-consistent Green's function method [24–26], and the Brueckner-Hartree-Fock (BHF) approach [27]. Within different approaches, the main features of the spectral functions turn out to have similar behavior in the region relevant to the short-range correlations. However, discrepancies of the predicted spectral functions based on different methods are still present and controversial interpretations of the experimental data exist [28]. Besides, the information about the nuclear spectral function and the effects of NN correlations in finite nuclear systems have also been explored in theory [29–33]. In Ref. [30], the authors pointed out that the effects of short-range correlations are insensitive to the bulk structure of the nuclear system by a comparison of the spectral function derived from experimental data with the one obtained from the Green's function method in nuclear matter, while only the spectral function of ^{12}C was reported without a systematic investigation for different nuclei. Within the framework of Correlated Basis Function approach, the scaled proton spectral function, i.e., the proton spectral function scaled by the number of protons, was compared for different nuclei and a significant increase of the scaled spectral function with the mass number was observed. In Ref. [34], experimental results of electron scattering on nuclei are available for several nuclei (^{12}C , ^{27}Al , ^{56}Fe and ^{197}Au) and the spectral function was explained as an indication of short-range correlations. In Ref. [23], the author calculated the spectral functions of the four nuclei (^{12}C , ^{27}Al , ^{56}Fe and ^{197}Au) in the self-consistent T-matrix approach and the target dependence of the scaled proton spectral function is expected to stem partially from the asymmetry of target and the density dependence of the spectral function by using a local density approximation (LDA). However, the effect of the density dependence of the spectral function on the target dependence of the scaled spectral function was not illustrated explicitly and the reason for the significant difference of the spectral functions going from ^{12}C to ^{197}Au was not explained. In our previous research, the extended BHF approach has been adopted

* Corresponding author: yinpeng@impcas.ac.cn

† Corresponding author: shangxinle@impcas.ac.cn

‡ Corresponding author: zuowei@impcas.ac.cn

to calculate the spectral functions in symmetric as well as asymmetric nuclear matter, and the three-body force effect on the spectral function in nuclear matter has been investigated [36, 37]. In the present paper, the extended BHF approach supplemented by the LDA will be firstly applied to calculate the spectral functions in finite nuclei. One of our purposes in the present paper is to investigate the strong target dependence of the scaled proton spectral function within the framework of the extended BHF approach.

In the present paper, we shall calculate the scaled spectral function from the LDA [38]. The calculation for finite nuclei and nuclear matter shall be performed within the framework of the Skyrme-Hartree-fock (SHF) method and the extended BHF approach, respectively. In this paper, only the spectral functions of the four nuclei, i.e., ^{12}C , ^{27}Al , ^{56}Fe and ^{197}Au are calculated while similar calculations can be naturally applied and extended to other nuclei.

The present paper is organized as follows. In the next section, we give a brief review of the adopted theoretical approaches including the extended BHF theory and a microscopic three-body force (TBF) model. We also give definitions and the corresponding physical interpretations of the mass operator and spectral function. In Section III, the calculated results will be reported and discussed. Finally, a summary is given in Section IV.

II. THEORETICAL APPROACHES

The present calculations are based on the extended BHF approach for asymmetric nuclear matter [39]. Here for completeness, we simply give a brief review about this theory. The starting point of the BHF approach is to obtain the reaction G -matrix by solving the following isospin dependent Bethe-Goldstone (BG) equation [40],

$$G(\rho, \beta; \omega) = V_{NN} + V_{NN} \sum_{k_1 k_2} \frac{|k_1 k_2\rangle Q(k_1, k_2) \langle k_1 k_2|}{\omega - \epsilon(k_1) - \epsilon(k_2)} G(\rho, \beta; \omega) \quad (1)$$

where $k_i \equiv (\vec{k}_i, \sigma_i, \tau_i)$ denotes the momentum, the z -component of spin and isospin of a nucleon, respectively. $Q(k_1, k_2) = [1 - n_0(k_1)][1 - n_0(k_2)]$ is the Pauli operator which prevents two nucleons in intermediate states from being scattered into their respective Fermi seas (Pauli blocking effect). Here $n_0(k)$ denotes the Fermi distribution function and it is given by a step function at zero temperature, i.e., $n_0(k) = \theta(k_F - k)$. The asymmetry parameter β is defined as $\beta = (\rho_n - \rho_p)/\rho$, where ρ , ρ_n and ρ_p denote the total nucleon, neutron and proton number densities, respectively. V_{NN} is the bare NN interaction and ω is the starting energy. $\epsilon(k)$ is the single-particle (s.p.) energy which is given by: $\epsilon(k) = \hbar^2 k^2 / (2m) + U(k)$. Here the auxiliary s.p. potential $U(k)$ controls the convergent rate of the hole-line expansion [40] and the continuous choice for the auxiliary potential is adopted in the present calculation since it provides a much faster convergence of the hole-line expansion up to high densities than the gap choice [41]. Under the continuous choice, the s.p. potential describes physically at the lowest BHF level the nuclear mean field felt by a nucleon in nuclear medium [42] and is calculated as follows:

$$U(k) = \text{Re} \sum_{k' \leq k_F} \langle k k' | G[\rho, \epsilon(k) + \epsilon(k')] | k k' \rangle_A, \quad (2)$$

where the subscript A denotes anti-symmetrization of the matrix elements.

In the present calculation, we adopt the Argonne V_{18} (AV18) two-body interaction [43] plus a microscopic TBF [44] constructed by using the meson-exchange current approach [45] for the realistic NN interaction V_{NN} . In the TBF model adopted here, the most important mesons, i.e., π , ρ , σ and ω have been considered. The parameters of the TBF model, i.e., the coupling constants and the form factors, have been self-consistently determined to reproduce the AV18 two-body force using the one-boson-exchange potential model and their values can be found in Ref. [44]. In our calculation, the TBF contribution has been included by reducing the TBF to an equivalently effective two-body interaction according to the standard scheme as described in Ref. [45]. The extension of the BHF scheme to include microscopic three-body forces can be found in Ref. [44–46]. In r -space, the equivalent two-body force V_3^{eff} reads:

$$\begin{aligned} \langle \vec{r}_1' \vec{r}_2' | V_3^{\text{eff}} | \vec{r}_1 \vec{r}_2 \rangle &= \frac{1}{4} \text{Tr} \sum_n \int d\vec{r}_3 d\vec{r}_3' \phi_n^*(\vec{r}_3') (1 - \eta(r_{13}')) (1 - \eta(r_{23}')) \\ &\times W_3(\vec{r}_1' \vec{r}_2' \vec{r}_3' | \vec{r}_1 \vec{r}_2 \vec{r}_3) \phi_n(\vec{r}_3) (1 - \eta(r_{13})) (1 - \eta(r_{23})). \end{aligned} \quad (3)$$

Within the framework of the Brueckner-Bethe-Goldstone theory, the mass operator can be expanded in a perturbation series according to the number of hole lines, i.e.,

$$M^\tau(k, \omega) = M_1^\tau(k, \omega) + M_2^\tau(k, \omega) + M_3^\tau(k, \omega) + \dots \quad (4)$$

where τ denotes neutron or proton (hereafter we will write out explicitly the isospin index τ). The mass operator is complex quantity, i.e., $M^\tau(k, \omega) = V^\tau(k, \omega) + iW^\tau(k, \omega)$ and the real part of its on-shell value can be identified with the potential energy felt by a neutron or a proton in asymmetric nuclear matter. In the present calculation, we consider the first two terms $M_1^\tau(k, \omega)$ and $M_2^\tau(k, \omega)$. $M_1^\tau(k, \omega)$ corresponds to the standard BHF s.p. potential. $M_2^\tau(k, \omega)$ is called the Pauli rearrangement term which describes the effects of the ground-state two-hole correlations on the s.p. potential [47, 48]. The detailed expressions for $M_1^\tau(k, \omega)$ and $M_2^\tau(k, \omega)$ can be found in Refs. [39]. According to the Lehmann representation for the Green function $G^\tau(k, \omega) = [\omega - k^2/2m - M^\tau(k, \omega)]^{-1}$, the nucleon spectral functions in nuclear matter can be expressed as follows, i.e.,

$$A^\tau(k, \omega) = -\frac{1}{\pi} \frac{W^\tau(k, \omega)}{[\omega - k^2/2m - V^\tau(k, \omega)]^2 + [W^\tau(k, \omega)]^2}, \quad (5)$$

and it fulfils the sum rule of $\int_{-\infty}^{\infty} A^\tau(k, \omega) d\omega = 1$.

One of the main purposes of the present work is to investigate the proton spectral functions of the finite nuclei system. To simplify the calculation, we adopt the spherical assumption for nuclei and the LDA has been applied. The proton spectral function for a finite nucleus is calculated by the radial integral of the proton spectral function in nuclear matter, and the expression reads

$$S^p(k, E) = \frac{2}{(2\pi)^3} \int A_h^p[\rho(r), \beta(r); k, E] d^3\vec{r}, \quad (6)$$

where $\rho(r)$ and $\beta(r)$ are the local density and isospin asymmetry at radius r , respectively. $A_h^p[\rho(r), \beta(r); k, E]$ is the proton hole spectral function in nuclear matter. The proton exciting energy is obtained by $E = \omega_F[\rho(r), \beta(r)] - \omega[\rho(r), \beta(r)]|_{\omega < \omega_F}$, where ω_F is the Fermi energy of nuclear matter.

III. RESULTS AND DISCUSSIONS

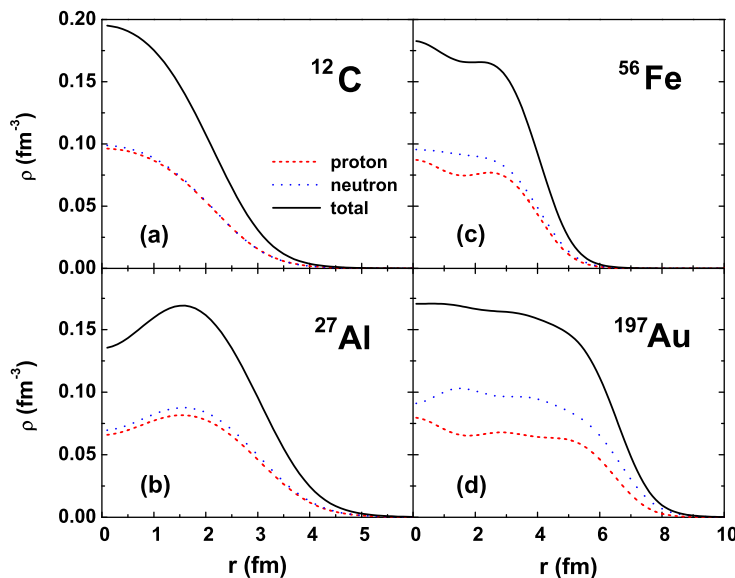


FIG. 1: Radial density distribution of the four nuclei ^{12}C (a), ^{27}Al (b), ^{56}Fe (c) and ^{197}Au (d) calculated by the SHF method with the LNS1 parameter set. The solid lines denote the total densities while the dashed and dotted lines represent the proton and neutron densities respectively.

To perform the LDA, in Fig.1 we display the neutron, proton and total density distributions of the four nuclei ^{12}C (a), ^{27}Al (b), ^{56}Fe (c) and ^{197}Au (d) which are calculated by the SHF method. We adopt the LNS1 parameter set which is obtained by fitting the properties of asymmetric nuclear matter predicted by the BHF approach [49]. This

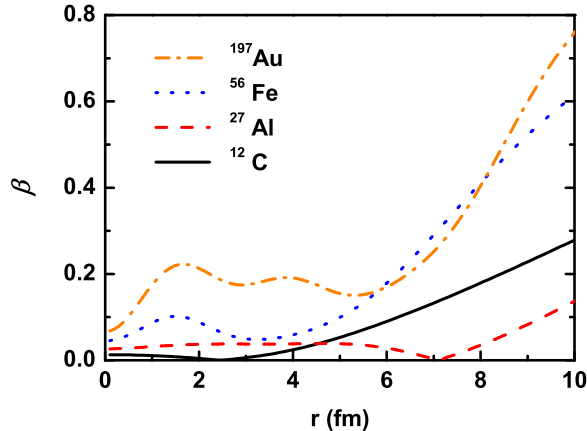


FIG. 2: Asymmetry distribution for the four nuclei ^{12}C (a), ^{27}Al (b), ^{56}Fe (c) and ^{197}Au (d) calculated by the SHF method with the LNS1 parameter set.

parameter set gives a satisfying description of properties of finite nuclei, such as binding energy and charge radius. One can find from Fig.1 that the total densities inside nuclei are not constant along the radii. For the heaviest nucleus ^{197}Au , the total density is found to be nearly constant in the central region and is close to the saturation density of nuclear matter. Besides, one has to know the asymmetry distributions inside nuclei for the application of the LDA. In Fig.2 we display the asymmetry distributions of the four nuclei ^{12}C , ^{27}Al , ^{56}Fe and ^{197}Au . The local asymmetry $\beta(r)$ is given by $[\rho_n(r) - \rho_p(r)]/[\rho_n(r) + \rho_p(r)]$, where $\rho_n(r)$ and $\rho_p(r)$ represent the neutron and proton densities at radius r , respectively. It is shown in Fig.2 that the asymmetries inside nuclei are not constant but have fluctuations along the radii. When the radii are not too large, i.e., the corresponding densities are not too small, the asymmetries can be roughly estimated by $(N - Z)/(N + Z)$, where N and Z are the neutron and proton numbers, respectively. However, the asymmetries of ^{56}Fe and ^{197}Au increase distinctly as the radii become very large, which is in accordance with the phenomenon of neutron skin or halo structure in nuclear physics.

One should notice that the LDA will give rise to uncertainties of calculations. In the recent BHF studies for finite nuclei, Bethe-Goldstone equation is solved directly for finite nuclei and several interesting new results were reported continuously[50–53]. For example, in Ref.[50], it has been shown that the different LDAs generate substantially different results by use of the same Brueckner theory with the same interaction adopted. Therefore, the investigation of the uncertainties caused by the LDA should be concerned in the future research.

From Fig.1 and Fig.2 one can know the density and asymmetry at radius r and consequently obtain the proton spectral function based on Eq.(6) for every nucleus discussed above. In Fig.3, we display the spectral functions divided by the proton numbers for the four nuclei ^{12}C , ^{27}Al , ^{56}Fe and ^{197}Au at four different momenta 330 MeV (a), 410 MeV (b), 490 MeV (c) and 570 MeV (d). Besides, we also show the experimental results via $(e, e'p)$ at JLab[34] for comparison. One may notice that at low energies the present calculation can well reproduce the experimental result at small momenta, while the discrepancy between them becomes apparent with increasing the momentum since the effects of final state interaction (FSI) become significant at high momenta[3, 15, 35]. To include the FSI in future calculations is potentially able to eliminate the discrepancy between the theoretical and experimental results at high momentum. It is also shown in Fig.3 that the spectral functions from the present calculation decrease with missing energy while the ones from the experiment behave differently. This can be explained by the existence of the Δ -resonance in the experiment which is not considered in our calculation. The Δ -resonance appears at high missing energy and consequently enhances the spectral function, for example, sizable contributions from the excitation of the Δ -resonance enhance the spectral function of ^{12}C at missing energies above 150 MeV. The improvement of the calculated spectral functions at high missing energies is expected by inclusion of the Δ -resonance in future theoretical calculations.

In Ref. [23], the CD-Bonn interaction was used in the calculation and it is stated that to adopt a nuclear potential with a hard core could bring the calculation closer to the experimental results. In our calculation, the AV18 interaction is adopted, which introduces stronger short-range correlations than the CD-Bonn interaction. Besides, a microscopic TBF is included in our calculation, which also induces strong short-range correlations. Consequently, we find that

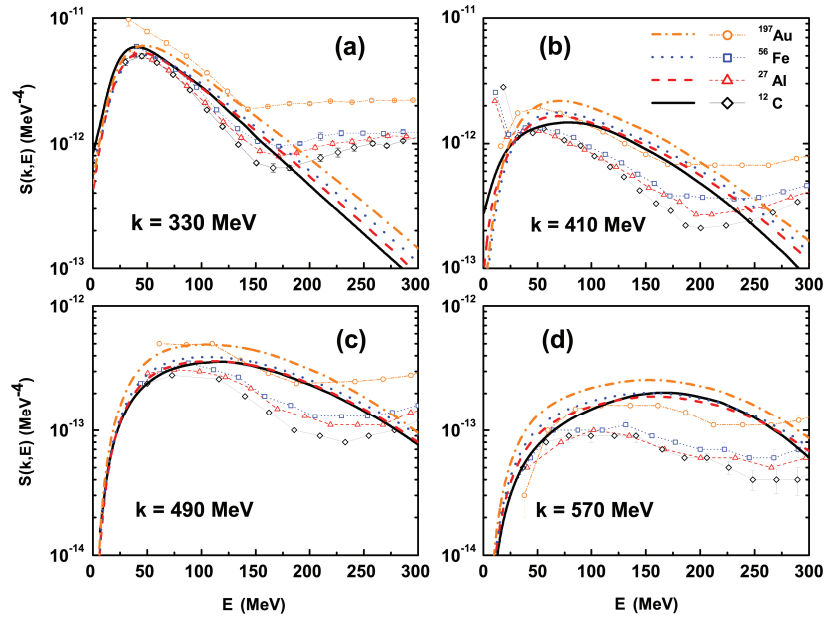


FIG. 3: By various lines we give spectral functions divided by proton numbers from our calculations for the four nuclei ^{12}C , ^{27}Al , ^{56}Fe and ^{197}Au at four different momenta 330 MeV (a), 410 MeV (b), 490 MeV (c) and 570 MeV (d). Open-symbol dots correspond to the experimental results taken from Ref.[34].

the spectral functions given by the AV18 interaction are larger than those given by the CD-Bonn interaction and our calculation gives a better description of the experimental results at low momentum. However, the present calculation still cannot give a quantitative description of the experimental results. To quantitatively reproduce the experimental results is still challenging for nuclear theory.

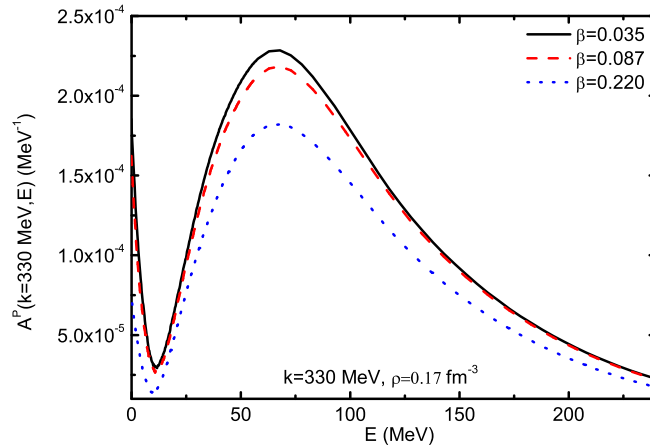


FIG. 4: Proton spectral function as a function of missing energy with momentum $k = 330$ MeV for three different asymmetries ($\beta = 0.035, 0.087$ and 0.22) at the saturation density in nuclear matter..

By comparing the four panels (a), (b), (c) and (d) in Fig.3, one can notice that the spectral function decreases with momentum for the same nucleus, which means that the possibility to find a nucleon inside a nucleus decreases by increasing the momentum. At a given momentum, one may notice from both the experimental results and our present calculations that the off-shell spectral function per proton increases when going from ^{12}C to ^{197}Au which is called the target dependence of the scaled proton spectral functions in finite nuclei. To understand this phenomenon, we start the discussion from the proton spectral function in nuclear matter.

Firstly, we show the proton spectral function in asymmetric nuclear matter as a function of the missing energy for three different asymmetries ($\beta = 0.035, 0.087$ and 0.22) at the saturation density in Fig.4. One can see from Fig.4 that the proton spectral function decreases with asymmetry of nuclear matter, which means that the probability to find a proton inside a nucleus decreases with asymmetry. This result is in accordance with our previous calculation [54] and can be explained by the tensor component of nucleon-nucleon interaction [55, 56]. However, one should notice that this asymmetry dependence is very weak. From Fig.2 we can find that the asymmetries of the central regions for these 4 nuclei are less than 0.22. Thus one can conclude that the asymmetry distributions inside finite nuclei has negligible effects on the target dependence of the scaled proton spectral functions of nuclei.

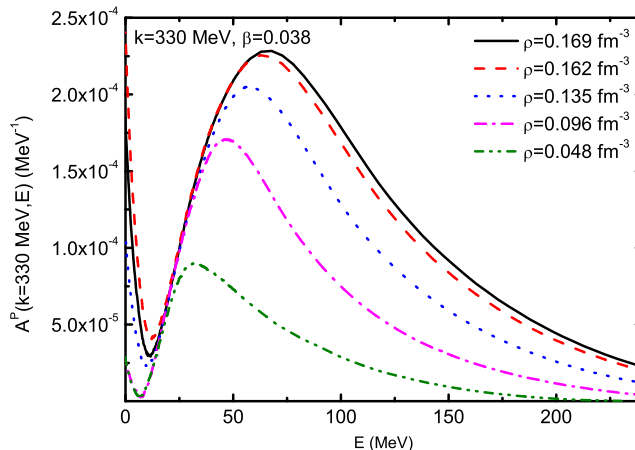


FIG. 5: Proton spectral function as a function of missing energy with momentum $k = 330$ MeV for five different densities ($\rho = 0.169, 0.162, 0.135, 0.096$ and 0.048 fm^{-3}) in nuclear matter with asymmetry $\beta = 0.038$.

Secondly, in Fig.5 we display the proton spectral function versus the missing energy at five different densities ($\rho = 0.169, 0.162, 0.135, 0.096$ and 0.048 fm^{-3}) in asymmetric nuclear matter at a fixed asymmetry of $\beta = 0.038$. The proton spectral function increases with density of nuclear matter since higher density induces stronger short-range correlations. One can expect from Eq.(6) that the nuclear spectral function increases with the range of the high density region in a nucleus (one should note that what are plotted in Fig.5 is for the total density and the proton density dependence is expected to have the similar behavior). Furthermore, according to Eq.(6), the scaled proton spectral functions of finite nuclei can be written as,

$$\frac{S^p(k, E)}{Z} \propto \frac{\int A_h^p[\rho(r), \beta(r); k, E] d^3 \vec{r}}{\int \rho_p(r) d^3 \vec{r}}. \quad (7)$$

Based on the above discussion, we can find that for a given nucleus, the right hand of Eq.(7) is mainly contributed by the proportion of the high density region of the proton. It implies a larger proportion of the high density region of the proton will generate a higher value of the scaled proton spectral function.

TABLE I: Proportions of the high density region of the proton, i.e. χ , and scaled proportions of the high density region of the proton, i.e. χ_C , for the four different nuclei ^{12}C , ^{27}Al , ^{56}Fe and ^{197}Au .

| Nuclei | χ | χ_C |
|-------------------|--------|----------|
| ^{12}C | 0.45 | 1.00 |
| ^{27}Al | 0.63 | 1.39 |
| ^{56}Fe | 0.68 | 1.49 |
| ^{197}Au | 0.76 | 1.67 |

To be more explicit, we define a quantity $\chi = \frac{\int_0^{r_h} \rho_p(r) d^3 \vec{r}}{\int \rho_p(r) d^3 \vec{r}}$, where r_h represents the range of the high density region of the proton, to signify the proportion of the high density region of the proton. In practice, r_h is defined according to the half value of the maximum proton density, i.e., $\rho_p(r_h) = \frac{\rho_p^{max}}{2}$. In Tab.I, in the second column we display χ

for the four different targets considered in the present paper, i.e. ^{12}C , ^{27}Al , ^{56}Fe and ^{197}Au . In the third column of the Tab.I, we show the scaled proportions of the high density region of the proton χ_C , which is defined by $\chi_C = \frac{\chi_i}{\chi_{^{12}\text{C}}}$ where i runs over ^{12}C , ^{27}Al , ^{56}Fe and ^{197}Au . From Tab.I we can see that the proportion of the high density region of the proton increases significantly going from ^{12}C to ^{197}Au , which is in accordance with the target-dependent behavior of the scaled proton spectral function in Fig.3. The role of χ in the target dependence of the scaled proton spectral function is more pronounced than the one of $\frac{N+Z}{Z}$, which was stressed in Ref. [23]. We conclude that the proportion of the high density region of the proton plays a crucial role in the target-dependent behavior of the scaled proton spectral function.

IV. SUMMARY

In summary, we have calculated the proton spectral functions for finite nuclei by the local density approximation where the nuclear structure is calculated from the Skyrme-Hartree-Fock method and the nuclear matter calculation is performed within the framework of the extended Brueckner-Hartree-Fock approach by adopting the AV18 two-body interaction supplemented with a microscopic three-body force. Our calculation is in good accordance with the experimental results at small momenta. Besides, the absence of the Δ -resonance in our calculation leads to a discrepancy with the experimental results at high missing energies. From our calculation, we also find that the scaled proton spectral function increases when going from ^{12}C to ^{197}Au , which is consistent with the experimental results. In asymmetric nuclear matter, the effects of short-range correlations increase with density and hence the spectral function becomes larger at higher densities. By a further investigation, we find that the proportion of the high density region of proton plays a significant role in the target dependence of the scaled proton spectral function. Inclusion of the Δ -resonance in nucleon-nucleon interaction as well as the final state interaction are expected to improve our results in future calculations [57]. In addition, the effects of the local density approximation on spectral functions of finite nuclei should also be investigated in the following research.

Acknowledgments

The authors appreciate valuable suggestions from Dr. Daniela Kiselev (-Rohe). Peng Yin appreciates the kind hospitality of Professor James P. Vary during his visit to Iowa State University. The work is supported by the National Natural Science Foundation of China (11435014, 11175219, 11373038, 11603046, 11705240, 11505241), the 973 Program of China (Grant No. 2013CB834405), the Strategic Priority Research Program The Emergence of Cosmological Structures of the Chinese Academy of Sciences, Grant No. XDB09000000, National Key R&D Program of China No. 2017YFA0402600, Guizhou Provincial Key Laboratory of Radio Astronomy and Data Processing, Guizhou Normal University, Guiyang 550001, China and the Knowledge Innovation Project (KJCX2-EW-N01) of the Chinese Academy of Sciences. This work is also partially supported by the CUSTIPEN (China-U.S. Theory Institute for Physics with Exotic Nuclei) funded by the U.S. Department of Energy, Office of Science under Grant No. de-sc0009971.

-
- [1] R. Schiavilla, R. B. Wiringa, S. C. Pieper, and J. Carlson, Phys. Rev. Lett. **98**, 132501 (2007).
 - [2] O. Buss, T. Gaitanos, K. Gallmeister, H. van Hees, M. Kaskulov, O. Lalakulich, A. B. Larionov, T. Leitner, J. Weil, and U. Mosel, Phys. Rep. **512**, 1 (2012).
 - [3] L. Frankfurt, M. Sargsian, and M. Strikman, Int. J. Mod. Phys. A **23**, 2991 (2008).
 - [4] J. M. Cavedon, B. Frois, D. Goutte, *et al.*, Phys. Rev. Lett. **49**, 978 (1982).
 - [5] V. R. Pandharipande, I. Sick and P. K. A. deWitt Huberts, Rev. Mod. Phys. **69**, 981 (1997).
 - [6] A. Ramos, A. Polls, and W. H. Dickhoff, Nucl. Phys. **A503**, 1 (1989).
 - [7] W. H. Dickhoff and M. Mütter, Rep. Prog. Phys. **55**, 1947 (1992).
 - [8] W. Dickhoff and C. Barbieri, Prog. Part. Nucl. Phys. **52**, 377 (2004).
 - [9] P.K.A. deMitt Huberts, J. Phys. **G16**, 507 (1990).
 - [10] L. Lapikás, J. Wesseling, and R. B. Wiringa, Phys. Rev. Lett. **82**, 4404 (1999).
 - [11] R. Starink *et al.*, Phys. Lett. **B474**, 33 (2000).
 - [12] M. F. van Batenburg, Ph. D. thesis, University of Utrecht (2001).
 - [13] D. Rohe *et al.*, Phys. Rev. Lett. **93**, 182501 (2004).
 - [14] R. A. Niyazov *et al.*, Phys. Rev. Lett. **92**, 052303 (2004); K. S. Egiyan *et al.*, Phys. Rev. Lett. **96**, 082501 (2006).
 - [15] F. Benmokhtar *et al.*, Phys. Rev. Lett. **94**, 082305 (2005); R. Shneur *et al.*, Phys. Rev. Lett. **99**, 072501 (2007).

- [16] J. L. S. Aclander *et al.*, Phys. Lett. B **453**, 211 (1999); A. Tang *et al.*, Phys. Rev. Lett. **90**, 042301 (2003); E. Piasetzky *et al.*, Phys. Rev. Lett. **97**, 162504 (2006).
- [17] C. J. G. Onderwater *et al.*, Phys. Rev. Lett. **81**, 2213 (1998).
- [18] L. A. Riley, P. Adrich, T. R. Baugher, *et al.* Phys. Rev. C **78**, 011303 (2008).
- [19] R. Subedi, R. Shneor, P. Monaghan, *et al.*, Science **320** (2008) 1476 and reference therein.
- [20] W. H. Dickhoff, Phys. Rep. **242**, 119 (1994).
- [21] E. N. E. van Dalen and H. Mütter, Phys.Rev.C **82**, 014319 (2010).
- [22] P. Konrad, H. Lenske, and U. Mosel, Nucl. Phys. A **756**, 192 (2005).
- [23] P. Božek, Phys. Lett. B **586**, 239 (2004).
- [24] T. Frick and H. Mütter, Phys. Rev. C **68**, 034310 (2003).
- [25] A. Rios, A. Polls, and I. Vidana, Phys.Rev.C **79**, 025802 (2009); A. Rios, A. Polls, and W. H. Dickhoff, *ibid.* **79**, 064308 (2009).
- [26] T. Frick, H. Mütter, A. Rios, A. Polls, and A. Ramos, Phys. Rev. C **71**, 014313 (2005).
- [27] Kh. S. A. Hassaneen and H. Mütter, Phys. Rev. C **70**, 054308 (2004).
- [28] M. Baldo and L. Lo Monaco, Phys. Lett. B **525**, 261 (2002).
- [29] H. Mütter, W.H. Dickhoff, Phys. Rev. C **49**, R17 (1994).
- [30] T. Frick, Kh. S. A. Hassaneen, D. Rohe, and H. Mütter, Phys. Rev. C **70**, 024309 (2004).
- [31] H. Mütter, A. Polls, W.H. Dickhoff, Phys. Rev. C **51**, 3040 (1995).
- [32] O. Benhar, A. Fabrocini, S. Fantoni, I. Sick, Nucl. Phys. A **579**, 493 (1994).
- [33] H. Mütter, G. Knehr, A. Polls, Phys. Rev. C **52**, 2955 (1995).
- [34] D. Rohe, Eur. Phys. J. **A 17**, 439 (2003).
- [35] C. Barbieri, L. Lapikás, D. Rohe, Eur. Phys. J. **A 34**, 85 (2005).
- [36] Pei Wang, Sheng-xin Gan, Peng Yin, Wei Zuo, Phys. Rev. C **87**, 014328 (2013).
- [37] Pei Wang and Wei Zuo, Phys. Rev. C **89**, 054319 (2014).
- [38] D. Van Neck and A. E. L. Dieperink, Phys. Rev. C **51**, 1800 (1995).
- [39] W. Zuo, I. Bombaci and U. Lombardo, Phys. Rev. C **60**, 024605 (1999).
- [40] B. D. Day, Rev. Mod. Phys. **50**, 495 (1978).
- [41] H. Q. Song, M. Baldo, G. Giansiracusa, and U. Lombardo, Phys. Rev. Lett. **81**, 1584 (1998); M. Baldo, A. Fiasconaro, H. Q. Song, G. Giansiracusa, and U. Lombardo, Phys. Rev. C **65**, 017303 (2002).
- [42] A. Lejeune, and C. Mahaux, Nucl. Phys. **A 295**, 189 (1978); R. Sartor, in *Nuclear Methods and the Nuclear Equation of State*, Ed. M. Baldo, (World Scientific, Singapore, 1999), Chapt.6.
- [43] R. B. Wiringa, V. G. J. Stoks and R. Schiavilla, *Phys. Rev. C* **51**, 38 (1995).
- [44] W. Zuo, A. Lejeune, U. Lombardo, and J.-F. Mathiot, Nucl. Phys. **A 706**, 418 (2002).
- [45] P. Grangé, A. Lejeune, M. Martzolff, and J.-F. Mathiot, Phys. Rev. C **40**, 1040(1989).
- [46] W. Zuo, A. Lejeune, U. Lombardo, and J.-F. Mathiot, Eur. Phys. J. **A 14**, 469 (2002).
- [47] M. Baldo, I. Bombaci, G. Giansiracusa, U. Lombardo, C. Mahaux and R. Sartor, Phys. Rev. C **41**, 1748 (1990).
- [48] M. Baldo, I. Bombaci, L. S. Ferreira, G. Giansiracusa, U. Lombardo, Phys. Lett. **209**, 135 (1988); Phys. Lett. **215**, 19 (1988).
- [49] D. Gambacurta, L. Li, G. Colò, U. Lombardo, N. V. Giai and W. Zuo, Phys. Rev. C **84**, 024301 (2011).
- [50] Haozhao Liang, PoS INPC2016 (2017) 361.
- [51] Shihang Shen, Jinniu Hu, Haozhao Liang, Jie Meng, Peter Ring, and Shuangquan Zhang, Chin. Phys. Lett. **33**, 102103 (2016).
- [52] Shihang Shen, Haozhao Liang, Jie Meng, Peter Ring, and Shuangquan Zhang, Phys. Rev. C **96**, 014316 (2017); Phys. Rev. C **97**, 054312 (2018).
- [53] Shihang Shen, Haozhao Liang, Jie Meng, Peter Ring, and Shuangquan Zhang, Phys. Lett. B **778**, 344 (2018); Phys. Lett. B **781**, 227 (2018).
- [54] P. Yin, J. L. Li, P. Wang, and W. Zuo, Phys. Rev. C **87**, 014314 (2013).
- [55] Peng Yin, Jianmin Dong, Wei Zuo, Chin. Phys. **C41**, 114102 (2017).
- [56] A. Rios, A. Polls, I. Vidana, Phys. Rev. C **79**, 025802 (2009).
- [57] M. Piarulli, L. Girlanda, R. Schiavilla, R. Navarro Pérez, J. E. Amaro, and E. Ruiz Arriola, Phys. Rev. C **91**, 024003 (2015); R. Sartor, in *Nuclear Methods and the Nuclear Equation of State*, Ed. M. Baldo, (World Scientific, Singapore, 1999), Chapt.4.